$\mathcal{H}$-Matrix Accelerated Contour Integral Method for Modeling Multiconductor Transmission Lines

Yu Zhao, *Student Member, IEEE*, Min Tang, *Member, IEEE*, Shang Xiang, and Junfa Mao, *Fellow, IEEE*

***Abstract*—An efficient algorithm based on the contour integral method (CIM) is presented in this letter for the modeling of lossy multiconductor transmission lines. Different from the volume integral equation, the CIM only discretizes the contour of the cross section of each conductor, which significantly reduces the number of unknowns in the resultant system equations. The solution of the CIM is accelerated by the hierarchical-matrix ($\mathcal{H}$-matrix) algorithm for the extraction of the per-unit-length resistance and inductance parameters of massively coupled transmission lines. The procedures for the $\mathcal{H}$-matrix-based solution are optimized to keep its optimal computational complexity. The numerical results from the proposed method agree well with those from the commercial software. The complexities of CPU time and memory cost for the construction of the $\mathcal{H}$-matrices are both $O(N \log N)$, and the complexity of the solution for parameter extraction is $O(N \log^2 N)$.**

***Index Terms*—Contour integral method (CIM), $\mathcal{H}$-matrix, multiconductor transmission lines, parameter extraction.**

I. Introduction

THE transmission line model is widely used in interconnects, power delivery networks, and other structures in high-speed digital systems for the analysis of signal integrity and power integrity. As the integration density of the advanced circuits grows consistently, accurate and efficient modeling for broadband characterization of lossy multiconductor transmission lines is more challenging.

The volume electric field integral equation based method of moments (MoM) gained the popularity in discretizing only the source region [1]. The surface-volume-surface electric field integral equation takes advantage of the transformation relationship between the surface current and the volumetric current [2]. However, the exorbitant number of volumetric meshes to guarantee the accuracy at high frequency makes the computation extremely expensive. The contour integral method (CIM) attracts more attention due to the elimination of the volumetric mesh. In [3], the potential functions act as the intermediate variables to compute the per-unit-length impedance. The equivalent surface impedance was derived based on CIM to combine with surface integral equation for modeling 3-D interconnects [4]. The CIM was further extended for the modeling of inhomogeneous material with a domain decomposition technique [5]. However, direct MoM solution to CIM would also become computationally prohibitive as the scale of the problem grows larger.

In this letter, an efficient algorithm based on the CIM is presented for the modeling of massively coupled transmission lines. To avoid the $O(N^2)$ complexity for the construction of system equations and $O(N^3)$ complexity for the matrix arithmetics, the $\mathcal{H}$-matrix-based algorithms [6] are adopted to accelerate the solution of CIM. In Section II, the Green's identity based CIM and the basic MoM solution are presented. In Section III, the $\mathcal{H}$-matrix-based solution for efficient parameter extraction are then developed. Procedures for the $\mathcal{H}$-based arithmetics are optimized to adapt to the special requirements of CIM as well as reach the optimal complexity of $\mathcal{H}$-matrix. The accuracy and efficiency of the proposed method are demonstrated in Section IV, followed by the conclusion in Section V.

II. Basic Formulations

A. Contour Integral Method

Consider a system of M-conductor transmission lines located in nonmagnetic uniform dielectrics along z-axis. Under the quasi-TM assumption, the interior tangential electric field E_z of the pth conductor is governed by the 2-D Helmholtz equation

$$\nabla^2 E_z(\boldsymbol{\rho}) - j\omega\mu_0\sigma^{(p)} E_z(\boldsymbol{\rho}) = j\omega\mu_0\sigma^{(p)} \frac{\partial V^{(p)}}{\partial z}, \boldsymbol{\rho} \in S^{(p)} \tag{1}$$

where ω is the angular frequency, μ_0 is the permeability, and $\sigma^{(p)}$ and $S^{(p)}$ are the conductivity and cross section of the pth conductor, respectively. The right-hand side of (1) is treated as the excitation field, and $V^{(p)}$ is the electric potential.

According to the Green's second identity, E_z can be represented by the integration along the contour of the conductor,

$$E_z(\boldsymbol{\rho}) = \oint_{l^{(p)}} \left[G_p(\boldsymbol{\rho}, \boldsymbol{\rho}') \frac{\partial E_z(\boldsymbol{\rho}')}{\partial n} - E_z(\boldsymbol{\rho}') \frac{\partial G_p(\boldsymbol{\rho}, \boldsymbol{\rho}')}{\partial n} \right] \mathrm{d}l' - \frac{\partial V^{(p)}}{\partial z} \left[1 + \oint_{l^{(p)}} \frac{\partial G_p(\boldsymbol{\rho}, \boldsymbol{\rho}')}{\partial n} \mathrm{d}l' \right], \boldsymbol{\rho} \in S^{(p)} \tag{2}$$

where $G_p(\boldsymbol{\rho}, \boldsymbol{\rho}') = -\frac{j}{4} H_0^{(2)}(k^{(p)}|\boldsymbol{\rho} - \boldsymbol{\rho}'|)$ is the Green's function of 2-D Helmholtz equation, $H_0^{(2)}$ is the second-kind Hankel function of the zeroth order, $k^{(p)} = \sqrt{-j\omega\mu_0\sigma^{(p)}}$ is the wave number inside the pth conductor material, $\boldsymbol{\rho}$ and $\boldsymbol{\rho}'$ are the observation and source points, respectively, and $l^{(p)}$ is the contour

Manuscript received May 22, 2017; accepted June 13, 2017. Date of publication July 18, 2017; date of current version November 3, 2017. This work was supported by the National Science Foundation of China under Grant 61234001 and Grant 61361166010 and the Science Challenge Program. *(Corresponding author: Min Tang.)*

The authors are with the Key Laboratory of Ministry of Education of Design and Electromagnetic Compatibility of High Speed Electronic Systems, Shanghai Jiao Tong University, Shanghai 200240, China (e-mail: zhaoyu775885@163.com; tm222@sjtu.edu.cn; bingoxiang917@sjtu.edu.cn; jfmao@sjtu.edu.cn).

Color versions of one or more of the figures in this letter are available online at http://ieeexplore.ieee.org.

Digital Object Identifier 10.1109/TEMC.2017.2722820

of the cross section $S^{(p)}$. The normal derivative denotes the external direction at the contour of the cross section.

In the exterior region of the conductors, the tangential electric field E_z satisfies the 2-D Laplace equation

$$\nabla^2 E_z(\boldsymbol{\rho}) = 0, \boldsymbol{\rho} \in S^c \tag{3}$$

where S^c represents the nonconductor region. Likewise for the exterior tangential electric field, we have

$$E_z(\boldsymbol{\rho}) = \oint_l \Big[-G_0(\boldsymbol{\rho},\boldsymbol{\rho}')\frac{\partial E_z(\boldsymbol{\rho}')}{\partial n} + E_z(\boldsymbol{\rho}')\frac{\partial G_0(\boldsymbol{\rho},\boldsymbol{\rho}')}{\partial n}\Big]\mathrm{d}l', \boldsymbol{\rho} \in S^c \tag{4}$$

where $G_0(\boldsymbol{\rho},\boldsymbol{\rho}') = -\frac{1}{2\pi}\ln(|\boldsymbol{\rho}-\boldsymbol{\rho}'|)$ is the Green's function of the 2-D Laplace equation, and l is the union of the contour of all the cross sections.

According to the Ampere's law, the current I_p along the pth conductor can be represented by the contour integration of the magnetic field strength $\boldsymbol{H}(\boldsymbol{\rho})$

$$I_p = \oint_{l^{(p)}} \boldsymbol{H}(\boldsymbol{\rho})\cdot \mathrm{d}\boldsymbol{l}' = \frac{1}{j\omega\mu_0}\oint_{l^{(p)}}\frac{\partial E_z(\boldsymbol{\rho})}{\partial n}\mathrm{d}l. \tag{5}$$

B. MoM Solution

The contour of the pth conductor is discretized by $N^{(p)}$ segments. The total number of segments is N, which is the sum of the $N^{(p)}, p = 1,\ldots,M$. The E_z and $\partial E_z/\partial n$ are expanded by the piecewise basis functions,

$$E_z(\boldsymbol{\rho}) = \sum_{p=1}^{M}\sum_{i=1}^{N^{(p)}} \alpha_i^{(p)} g_i^{(p)}(\boldsymbol{\rho}), \frac{\partial E_z}{\partial n} = \sum_{p=1}^{M}\sum_{i=1}^{N^{(p)}} \beta_i^{(p)} g_i^{(p)}(\boldsymbol{\rho}) \tag{6}$$

$$g_i^{(p)}(\boldsymbol{\rho}) = \begin{cases} 1, & \boldsymbol{\rho} \in l_i^{(p)} \\ 0, & \boldsymbol{\rho} \notin l_i^{(p)} \end{cases} \tag{7}$$

where $l_i^{(p)}$ represents both the ith segment of the pth conductor and the corresponding length, and

$$\begin{aligned} \boldsymbol{\alpha} &= \big[\alpha_1^{(1)},\ldots,\alpha_i^{(p)},\ldots,\alpha_{N^{(M)}}^{(M)}\big]^T \\ \boldsymbol{\beta} &= \big[\beta_1^{(1)},\ldots,\beta_i^{(p)},\ldots,\beta_{N^{(M)}}^{(M)}\big]^T \end{aligned} \tag{8}$$

are the coefficient vectors for E_z and $\partial E_z/\partial n$, respectively.

By eliminating the singular terms and adopting the point matching method, the resultant system equations are

$$\begin{aligned} \boldsymbol{T}_1\boldsymbol{\alpha} + \boldsymbol{T}_2\boldsymbol{\beta} &= \boldsymbol{T}_5\boldsymbol{U} \\ \boldsymbol{T}_3\boldsymbol{\alpha} + \boldsymbol{T}_4\boldsymbol{\beta} &= \boldsymbol{0}. \end{aligned} \tag{9}$$

The elements of $\boldsymbol{T}_i, i = 1,2,3,4$, are calculated by the contour integration in (2) and (4), and $\boldsymbol{T}_5$ is the diagonal matrix obtained by

$$\boldsymbol{T}_5 = \mathrm{diag}\{\boldsymbol{T}_1\cdot\boldsymbol{v}_N\} \tag{10}$$

where $\boldsymbol{v}_N$ is the N-dimensional full-one column vector.

Since the segments on the boundary of a conductor have identical potential, the excitation vector $\boldsymbol{U}$ can be represented by

$$\mathbf{U} = \boldsymbol{Q}\cdot\frac{\partial \mathbf{V}}{\partial z} \tag{11}$$

where $\mathbf{V} = \big[V_1,\ldots,V_p,\ldots,V_M\big]^T$ is the electric potential vector, and

$$\boldsymbol{Q} = \begin{bmatrix} \boldsymbol{v}_{N^{(1)}} & & & & \\ & \ddots & & & \\ & & \boldsymbol{v}_{N^{(p)}} & & \\ & & & \ddots & \\ & & & & \boldsymbol{v}_{N^{(M)}} \end{bmatrix}. \tag{12}$$

According to (5), the current vector is

$$\mathbf{I} = \big[I_1,\ldots,I_p,\ldots,I_M\big] = \frac{1}{j\omega\mu_0}\boldsymbol{P}\cdot\boldsymbol{\beta} \tag{13}$$

where

$$\boldsymbol{P} = \begin{bmatrix} \boldsymbol{v}_{N^{(1)}}^T\boldsymbol{P}^{(1)} & & & & \\ & \ddots & & & \\ & & \boldsymbol{v}_{N^{(p)}}^T\boldsymbol{P}^{(p)} & & \\ & & & \ddots & \\ & & & & \boldsymbol{v}_{N^{(M)}}^T\boldsymbol{P}^{(M)} \end{bmatrix} \tag{14}$$

and the matrices $\boldsymbol{P}^{(p)} = \mathrm{diag}\{l_i^{(p)}\}$ are formatted by the length of each segment on the pth conductor.

Based on the Telegrapher's equation, the electric potential vector $\mathbf{V}$ and the current vector $\mathbf{I}$ are related by

$$-\frac{\partial \mathbf{V}}{\partial z} = \big[\mathbf{R} + j\omega\mathbf{L}\big]\cdot\mathbf{I}. \tag{15}$$

The resistance and inductance matrices thus satisfy the following equation,

$$\mathbf{R} + j\omega\mathbf{L} = -j\omega\mu_0\Big(\boldsymbol{P}\cdot\boldsymbol{X}\cdot\boldsymbol{T}_5\cdot\boldsymbol{Q}\Big)^{-1} \tag{16}$$

where

$$\boldsymbol{X} = \big(\boldsymbol{T}_2 - \boldsymbol{T}_1\cdot\boldsymbol{T}_3^{-1}\cdot\boldsymbol{T}_4\big)^{-1}. \tag{17}$$

III. $\mathcal{H}$-Matrix-Based Solution

Direct MoM solution with $O(N^3)$ complexity is computationally prohibitive as N becomes large, which inspired us to adopt the efficient $\mathcal{H}$-matrix framework for the solution of CIM. According to the methodology of the $\mathcal{H}$-matrix, the basis functions are first clustered based on the spatial information. The interactions between clusters are identified as admissible and inadmissible block clusters by the admissibility condition, which judges the far-field and near-field groups according to the distances and the diameters of the clusters [6].

However, the conventional $\mathcal{H}$-matrix-based solution of CIM cannot reach the optimal complexity, due to the problems in two aspects:

1) The multiplication of $\mathcal{H}$-matrix $\boldsymbol{A}_{N\times N}$ and full-rank matrix $\boldsymbol{B}_{N\times M}$ is of complexity $O(NM\log N)$.
2) The sparsity of the intermediate full-rank matrices $\boldsymbol{P}$ and $\boldsymbol{Q}$ are not fully exploited.

A. Clustering Scheme

According to (11)–(14), $\boldsymbol{P}$ and $\boldsymbol{Q}$ are nearly block diagonal, except that the diagonal elements are block vectors, which means each row of $\boldsymbol{P}$ or each column of $\boldsymbol{Q}$ has only one nonzero

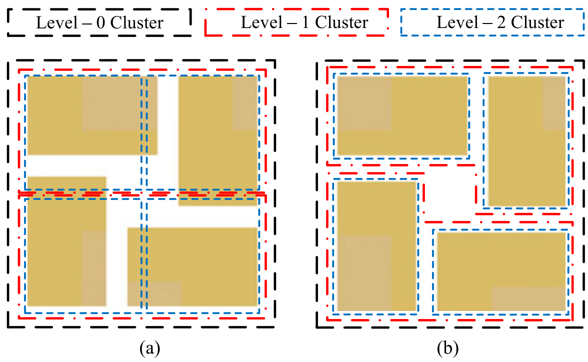

Fig. 1. Examples of the clustering method for the multiconductor transmission lines. (a) Conventional method. (b) Proposed method.

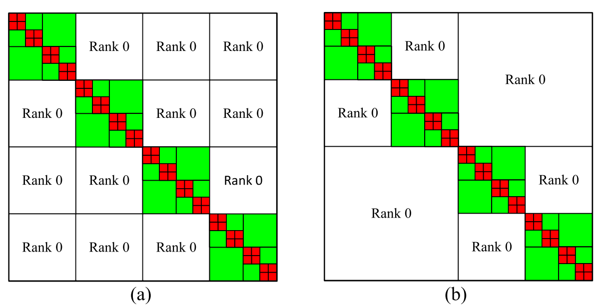

Fig. 2. Matrix layout of $\boldsymbol{T}_1$ and $\boldsymbol{T}_2$. (a) Set rank-0 matrices. (b) Merge rank-0 matrices.

block. The matrix-vector product (MVP) with the block vectors, named as the incomplete MVP, considers only the nonzero block, which proportionally reduces the number of operations.

Since the basis functions are regrouped, the MVP of $\mathcal{H}$-matrix also involves the permutation of the vector. We need a clustering scheme that keeps the properties of $\boldsymbol{P}$ and $\boldsymbol{Q}$ even with the permutation. In this respect, the basis functions belonging to the same conductor should be partitioned together. The proposed clustering scheme has the following two steps.

1) Individual conductors are clustered bisectionally level by level, until each cluster contains only one single conductor.
2) Basis functions belonging to each conductor are geometrically bisected, until the size of the cluster reaches the prefixed maximum size $n_{\max}$.

An example of the conventional and proposed clustering scheme is shown in Fig. 1.

B. Optimization of Low-Rank Compression

The inadmissible blocks correspond to full-rank matrices. The admissible blocks correspond to low-rank matrices, which can be built via the adaptive cross approximation (ACA) [7]. The reduced singular value decomposition (rSVD) is adopted to further compress the low-rank matrices. Both ACA and rSVD are performed with the prescribed threshold ϵ.

The coarsening of the $\mathcal{H}$-block merges small admissible blocks to generate larger blocks, which keeps the accuracy and ensures the feasibility in the meantime [8]. Besides, $\boldsymbol{T}_1$ and $\boldsymbol{T}_2$ are sparse system matrices, since no internal interactions exist between the basis functions on any two different conductors. The off-diagonal blocks that correspond to the interactions between

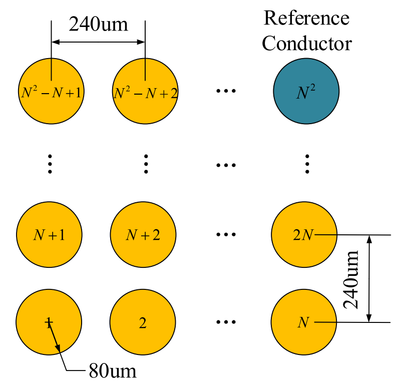

Fig. 3. Cross-sectional view of the transmission lines.

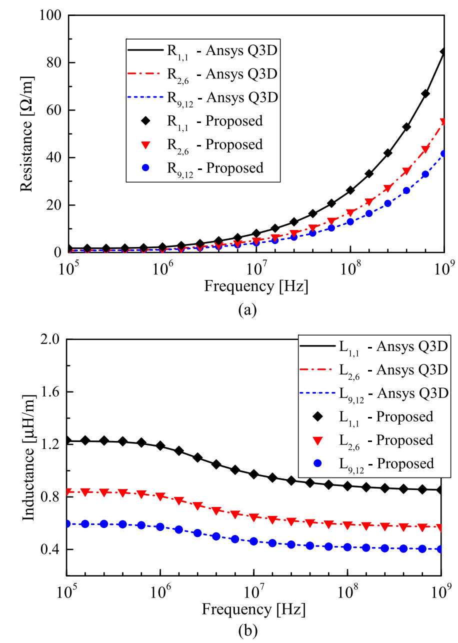

Fig. 4. Extraction of the resistance and inductance matrices for the 5×5 transmission lines. (a) Resistance parameters. (b) Inductance parameters.

different conductors are set to be rank-0 matrices, and merged level-by-level without the loss of precision, as shown in Fig. 2.

C. Computational Cost Analysis

The electrical size for the structures in high-speed systems are relatively small, thus the max rank of the low-rank matrices keeps nearly constant with the prescribed accuracy [9]. The CPU time and memory cost for the construction of the $\mathcal{H}$-matrices $\boldsymbol{T}_i, i = 1, 2, 3, 4$, have the optimal complexity of $O(N \log N)$ [6].

The intermediate matrix $\boldsymbol{X}$ involves the $\mathcal{H}$-based matrix-matrix product (MMP) and matrix inversion, both of which have the complexity of $O(N \log^2 N)$ [6]. The MMP of diagonal matrix $\boldsymbol{T}_5$ and $\boldsymbol{Q}$ requires only $O(N)$ operations, and does not change the structure of $\boldsymbol{Q}$. The number of operations for the multiplication of $\boldsymbol{X}$ and $\boldsymbol{Q}$ can be estimated by

$$\#\text{operation} = \sum_{p=1}^{M} O(N^{(p)} \log N) = O(N \log N). \tag{18}$$

which is the sum of incomplete MVP operations for the M columns. $\boldsymbol{P}$ and $\boldsymbol{Q}$ are very sparse matrices with only N nonzero

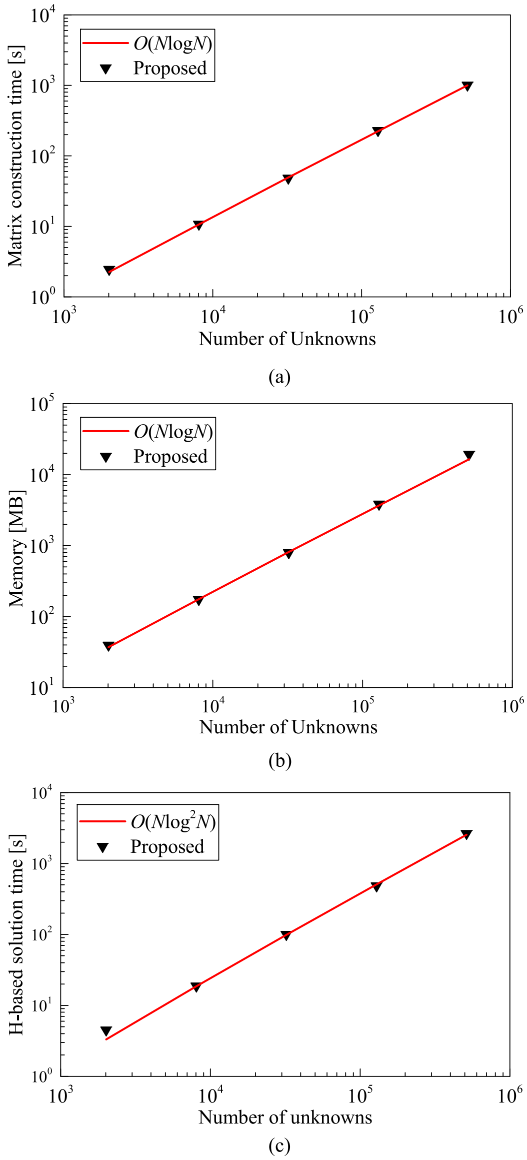

Fig. 5. Performance of the proposed method for simulating massively coupled transmission lines. (a) Matrix construction time. (b) Memory cost. (c) Solution time for parameter extraction.

elements. Therefore, the MMP with $\boldsymbol{P}$ or $\boldsymbol{Q}$ has the same cost as the MVP. Besides, the coarsening of $\mathcal{H}$-matrix has a complexity of $O(N \log N)$ [8]. Taken all the above into consideration, the overall computational complexity of the $\mathcal{H}$-matrix-based solution for parameter extraction is $O(N \log^2 N)$.

IV. Numerical Examples

In this section, the distributed resistance and inductance matrices of massively coupled transmission lines are extracted to show the accuracy and efficiency of the proposed method. The structure consists of an N-by-N cylinder conductor array. Conductors are labeled from 1 to N^2, and the N^2th conductor acts as the reference conductor, as shown in Fig. 3. The radius of each cylinder is 80 μm, and the pitch is 240 μm. The conductivity of each conductor is $\sigma = 5.72 \times 10^7$ S/m.

A. Validation of Accuracy

In the first example, we choose $N = 5$. Each conductor is discretized by 500 segments, thus the total number of segments is 12 500. The maximum size $n_{\max}$ for clustering is set to be 50, the admissible coefficient is 0.5, and the error threshold for both ACA and SVD is $\epsilon = 10^{-4}$. The numerical results, as shown in Fig. 4, are compared with those from the commercial software ANSYS Q3D [10], of which the 2-D solver is based on the finite element method (FEM). The relative errors of the extracted resistance and inductance parameters with respective to FEM validate the high accuracy of the proposed method.

B. Validation of Efficiency

In the second example, the size of the transmission lines varies as $N = 2, 4, 8, 16, 32$. All the parameters for $\mathcal{H}$-matrix and the scale of discretization are kept the same as those in the former example. The number of segments ranges from 2000 to 512 000. The simulation is performed at 1 GHz. The CPU time and memory cost are shown in Fig. 5. It can be observed that both the CPU time cost for matrix construction and memory cost have nearly $O(N \log N)$ complexity, and the solution time for parameter extraction has $O(N \log^2 N)$ complexity. The performance illustrated by the numerical example is in accordance with the theoretical analyses.

V. Conclusion

The $\mathcal{H}$-matrix accelerated CIM is presented for the modeling of massively coupled transmission lines. The procedures of the solution for parameter extraction are optimized to keep the optimal complexity of $\mathcal{H}$-matrix. Numerical examples demonstrate that the method provides similar precision as the commercial software. The complexities of the matrix construction and memory cost are $O(N \log N)$, and the complexity of the $\mathcal{H}$-matrix-based solution for parameter extraction is $O(N \log^2 N)$.

References

[1] M. Tsuk and J. Kong, "A hybrid method for the calculation of the resistance and inductance of transmission lines with arbitrary cross sections," *IEEE Trans. Microw. Theory Techn.*, vol. 39, no. 8, pp. 1338–1347, Aug. 1991.
[2] A. Menshov and V. Okhmatovski, "Surface-volume-surface electric field integral equation for magneto-quasi-static analysis of complex 3-d interconnects," *IEEE Trans. Microw. Theory Techn.*, vol. 62, no. 11, pp. 2563–2573, Nov. 2014.
[3] R. Wu and J. Yang, "Boundary integral equation formulation of skin effect problems in multiconductor transmission lines," *IEEE Trans. Magn.*, vol. 25, no. 4, pp. 3013–3015, Jul. 1989.
[4] Y. Zhao, F. Ling, and J. Mao, "Novel surface impedance modeling for broadband parameter extraction of 3-d interconnects," *IEEE Microw. Wireless Compon. Lett.*, vol. 27, no. 1, pp. 7–9, Jan. 2017.
[5] J. Preibisch, X. Duan, and C. Schuster, "An efficient analysis of power/ground planes with inhomogeneous substrates using the contour integral method," *IEEE Trans. Electromagn. Compat.*, vol. 56, no. 4, pp. 980–989, Aug. 2014.
[6] S. Börm, L. Grasedyck, and W. Hackbusch, "Hierarchical matrices," Lecture Note 21 of the Max Planck Institute for Mathematics in the Sciences, 2006.
[7] K. Zhao, M. Vouvakis, and J. Lee, "The adaptive cross approximation algorithm for accelerated method of moments computations of emc problems," *IEEE Trans. Electromagn. Compat.*, vol. 47, no. 4, pp. 763–773, Nov. 2005.
[8] L. Grasedyck, "Adaptive recompression of-matrices for BEM," *Computing*, vol. 74, no. 3, pp. 205–223, 2005.
[9] W. Chai and D. Jiao, "Fast $\mathcal{H}$-matrix-based direct integral equation solver with reduced computational cost for large-scale interconnect extraction," *IEEE Trans. Compon. Packag. Manuf. Technol.*, vol. 3, no. 2, pp. 289–298, Feb. 2013.
[10] ANSYS Q3D. ANSYS, Inc. [online]. Available: http://www.ansys.com